

## COLD WATER MODEL SIMULATION OF ALUMINUM LIQUID FLUCTUATIONS INDUCED BY ANODIC GAS IN NEW TYPE OF CATHODE STRUCTURE ALUMINUM ELECTROLYTIC CELL

Yan Liu, Ting'an Zhang, Zhihe Dou, Hongxing Wang, Guozhi Lv, Qiuyue Zhao, Naixiang Feng, Jicheng He  
School of Materials and Metallurgy of Northeastern University, Key Laboratory of Ecological Utilization of Multi-metal Intergrown  
Ores of Education Ministry, Shenyang, 110004, China

Keywords: new structure cathode, cold water model, anode gas

### Abstract

Compared to the conventional cathode structure electrolytic cell, the new type of cathode structure electrolytic cell can effectively inhibit the fluctuation of liquid aluminum, which can reduce the polar distance, decrease cell voltage, and save energy. A cold water model was designed according to scale of 1:3 with 160KA industrial electrolytic cell to examine aluminum liquid fluctuation induced by anodic gas in the new type of cathode structure electrolytic cell. High-speed photographs of the liquid interface waves show the effect of several cell parameters such as anode-cathode distance, electrolyte level, and gas flow rate. The study shows that in the new type of cathode structure electrolytic cell, the largest interface wave height will be reduced significantly.

### Introduction

In order to develop and verify theoretical models, physical models play an important role. In many industrial processes the conditions do not allow direct measurements of many parameters, and information which is crucial in order to verify a mathematical model cannot easily be obtained. The Hall-Heroult process for aluminum production is a typical example, due to the lack of flexibility and due to the highly corrosive high temperature system. Water model experiments of are commonly used to simulate aluminum electrolysis in industry.

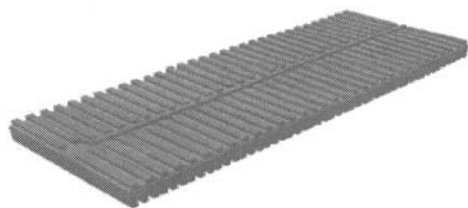


Fig. 1 Schematic Diagram of Cathode for new cathode structure

Figure 1 shows the structure of a new type of cathode reported by Feng et.al where the carbon block surface is not flat but with ridges. Characteristics of the electrolysis technology and operations for the new cathode structure aluminum reduction cell are as follows. The effective area for dissolved loss of cathode aluminum will be reduced due to stability improvement of cathode aluminum surface, so it can increase the current efficiency<sup>[1]</sup>.

This research includes three variations of new structure cathodes whose size is below.

Length×width×height ( mm ) :

570×70×60

570×80×60

570×90×60

High-speed photography was used to shoot the liquid surface waves for the two different cathode structures, varying anode cathode distance, electrolyte level, aluminum liquid level, and gas flow rate. The bubble images were analyzed by using special image analysis software (Image-Pro-Plus) and the maximum aluminum liquid fluctuation heights were obtained.

### Experimental Principle and Equipment

#### Water Model Principle

Geometrical Similarity Geometric similarity considers prototype and model similar in the main dimensions. Using water model made of glass instead of industrial aluminum cells, we use a model with water and vegetable oil to represent metal and bath, respectively, to study gas induced bath flow in the outer channel and the occurrence of waves at the metal-bath interface. The model and the prototype have the same proportion, but the water model is smaller than the prototype.

Fig. 2 shows the location of the three points 1 to 3, where interfacial deformations were measured. Also shown in the figure is the location of the origin and the unperturbed interface (horizontal black line). The size of physical model was designed according to scale of 1:3 with 160KA industrial electrolytic cell

Table 1 The size of physical model and the prototype

	Cell	Model
Anode size (mm)	1520×585×535	506×195×250
Cell area (mm)	8945×4220	2981×1406
Cell depth (mm)	600	560
Distance anode to endwall(mm)	450	150
Distance anode to sidewall (mm)	400	133
Center channel (mm)	280	94
Distance between anodes (mm)	45	15

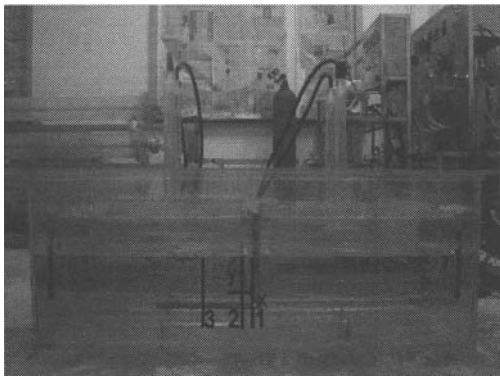
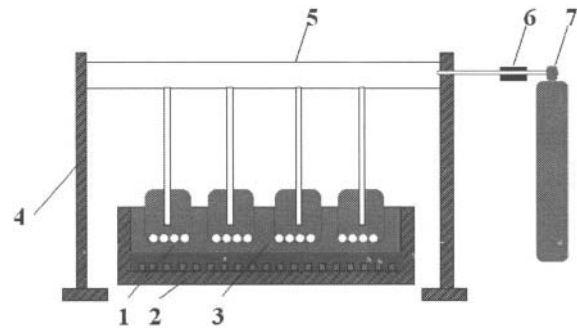


Fig. 2 Locations of the measurement points



1 Anode gas 2 Model of new cathode cell 3 Oil and water 4 Anode supporting device 5 Anode gas channels 6 Flow meter 7 Gas cylinder

Fig. 3 Sketch of Water model

**Dynamical Similarity** The physical properties of the fluids in a real cell are unfortunately difficult to match<sup>[2]</sup>. The molten metal phase in an industrial cell is characterized by a low viscosity and a high surface tension, properties which are not easily obtainable with common fluids. The fluids used in the current model are water to simulate the metal pad, light vegetable oil for the bath, and air for the gas formed under the anode. The oil–water combination is chosen to match the density and viscosity ratios as closely as possible, using safe and inexpensive room temperature fluids. A summary of the relevant parameters, compared with the industrial cell parameters (cell data from Chenosis and LaCamera<sup>[3]</sup> and Haarberg et al.<sup>[4]</sup>) is given in Table 2.

Table 2 Parameters of physical model and the prototype

Parameter	Model	Cell
$\rho_b$ , kg/m <sup>3</sup>	0.9	2.1
$\rho_m$ , kg/m <sup>3</sup>	1.0	2.3
$v_b$ , mm <sup>2</sup> /s	46.5	1.3
$v_m$ , mm <sup>2</sup> /s	1.0	0.4
$\sigma_{bm}$ , N/m	0.03	0.55
$\sigma_{bg}$ , N/m	0.02	0.14

Here,  $\rho_b$  is the density of bath and  $\rho_m$  is the density of molten metal.  $\nu_b$  is the kinematics viscosity of bath and  $\nu_m$  is the kinematics viscosity of bath.  $\sigma_{b,m}$ , and  $\sigma_{b,g}$  is the bath–metal and bath–gas surface tension, respectively.

As seen from Table 2, the parameters are entirely different from those encountered in a real cell. However, it is the combination of the mentioned parameters that determine whether dynamic similarity can be claimed. The bubble Froude number  $Fr_B$  is critical for an accurate representation of the bubbles. Fortunately, the Froude number can be defined from geometrical considerations as follows:

$$Fr_B = \frac{V_g^2}{gL} \quad [1]$$

Where  $v_g$  is the gas velocity,  $g$  is the acceleration of gravity, and  $L$  is the typical anode size. Hence, by choosing a 1:1 representation of the anode and the realistic gas rates, similarity can be claimed for  $Fr_B$ . As noted by Zhang et al<sup>[5]</sup> the effects of the other nondimensional groups are of secondary order. Here, the influences of viscosity and surface tension are grouped into a Morton number, defined as follows:

$$Mo = \frac{v_g^4 g \rho_b^3}{\sigma_{bg}} \quad [2]$$

Inserting values from Table 2 yields a factor of 500 in difference between the model and the cell Morton numbers. Though significant, it is not expected that this large difference is critical because the  $Fr_B$  will dominate the overall picture.

According to Solheim et al.,<sup>[6]</sup> the typical velocity in the interpolar is given as follows:

$$v_{int} \propto v_b^{-0.07} Mo^{-0.03} \quad [3]$$

Hence, one should expect that the bath velocities in the water model are up to 25 pct too low, compared with that in the cell. The interface deformation is assumed to be governed by its corresponding Froude number, defined as follows:

$$Fr_w = \frac{V}{c} \quad [4]$$

Where  $V$  is a characteristic velocity and  $c$  is a characteristic

wave propagation velocity. Assuming that the characteristic velocity is given by Eq. [3] and that the wave is both capillary and gravity driven,  $Fr_w$  is approximated as

$$Fr_w \propto \frac{v_b^{-0.07} Mo^{-0.03}}{\sqrt{\frac{g\lambda}{2\pi} \frac{\rho_m - \rho_b}{\rho_m + \rho_b} + \frac{2\pi\sigma}{\rho_m + \rho_b}} \lambda} \quad [5]$$

In Figure 4 the ratio  $Fr_w^{model}/Fr_w^{cell}$  is shown for the expected wavelengths.<sup>[7]</sup>

As seen from Figure 4, the Froude number in the model is over predicted for short wavelengths (because of the low surface tension) and under predicted for long wavelengths (because of the low density ratio). Over the expected range of wavelengths,  $Fr_w^{model}$  is  $\pm 25$  pct of the values expected in a real cell. Though not matched exactly, the parameters are believed to be close enough so that dynamic similarity can be claimed, at least for a narrow band of wavelengths.

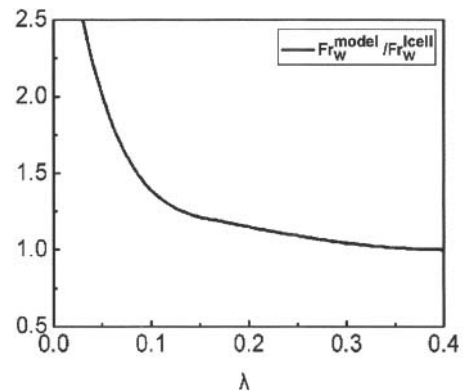


Fig. 4 The ratio  $Fr_w^{model}/Fr_w^{cell}$  for various wavelengths  $\lambda$ .

## Results and Discussion

### Comparison Aluminum Liquid Fluctuation of Conventional Cathode Structure Electrolytic Cell with the New Type of Cathode Structure Electrolytic Cell

Experimental condition: anode-cathode distance 3cm, electrolyte level 16cm, aluminum liquid level 17cm, gas flow rate  $1.0m^3/h$

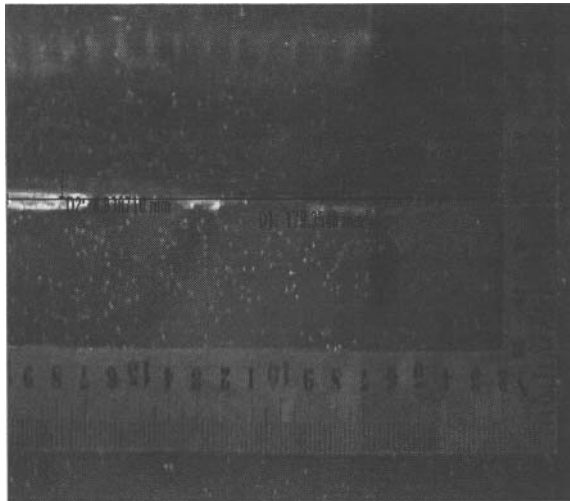


Fig. 5 Aluminum liquid fluctuation of new cathode structure electrolytic cell (After image analysis)

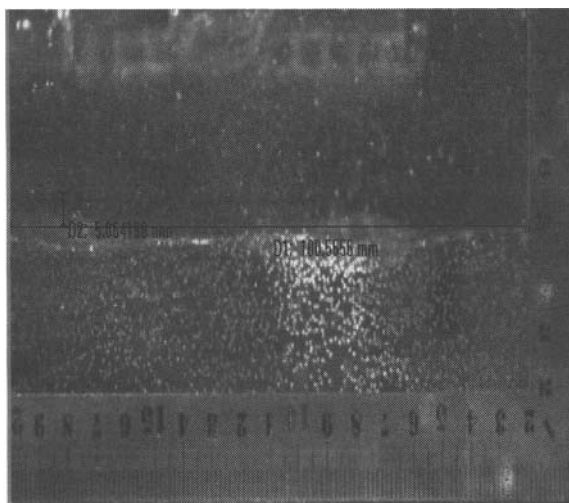


Fig. 6 Aluminum liquid fluctuation of conventional cathode structure electrolytic cell (After image analysis)

In the pictures (Figs 5 and 6), D1 is the liquid surface before experimental (standard line), and D2 is the maximum aluminum liquid fluctuation height at location 3.

From figs 5 and 6, we can see D2 is 4.8 mm in the new cathode model compared to 5.9mm in the conventional cell model.

Obviously , D2 is smaller when we use new cathode structure meaning that fluctuation is weakened and it may be possible to decrease cell voltage and save energy

### Effect of Operating Parameters on Aluminum Liquid Fluctuation in New Type of Cathode Structure Aluminum Electrolytic Cell

#### Effect of Gas Flow Rate on Aluminum Liquid Fluctuation

Experiment study on the effect of different gas flow rate on

aluminum liquid fluctuation, respectively is  $0.6\text{m}^3/\text{h}$ ,  $0.9\text{m}^3/\text{h}$ ,

$1.2\text{m}^3/\text{h}$ ,  $1.5\text{m}^3/\text{h}$

Experimental condition: anode-cathode distance 3cm, electrolyte level 14cm, aluminum liquid level 17cm

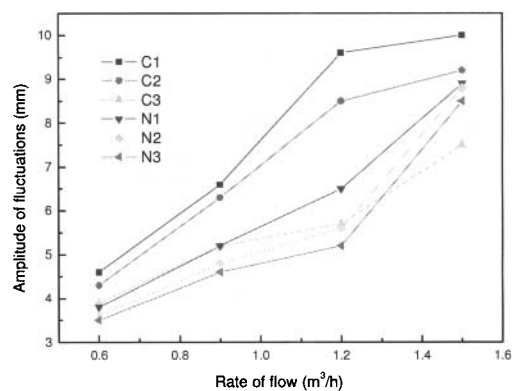


Fig.7 Effect of gas flow rate on the maximum aluminum liquid fluctuation height at different points

In figures 7-11, C means conventional cathode structure; N means new cathode structure, and the numbers 1-3 refer to locations where wave fluctuations were measured.

Analysis: As the gas flow rate increases, the liquid surface waves become more intense. The maximum aluminum liquid fluctuation height will increase in both types of cell, but the maximum fluctuation is greater for the conventional cell at all three locations.

#### Effect of Anode-cathode Distance (ACD) on Aluminum Liquid Fluctuation

Experiment study on the effect of different ACD on aluminum liquid fluctuation respectively is 3cm, 4cm, 5cm.

Experimental condition: electrolyte level 16cm, aluminum liquid level 17cm, gas flow rate  $1.0\text{m}^3/\text{h}$ .

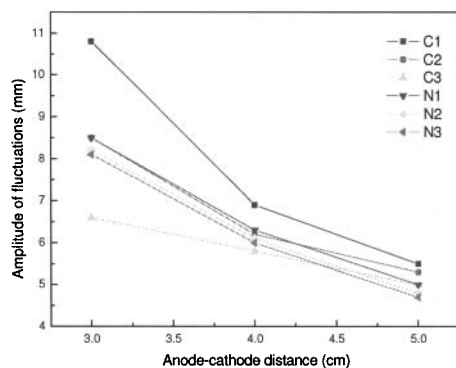


Fig. 8 Effect of ACD on fluctuation height

Analysis:

The change of slope is gentle as the ACD is reduced from 5 to 4 cm, but a larger slope appears between 3 and 4 cm. When ACD is 3cm, the fluctuation is very severe and the maximum fluctuation height is very large. With the ACD increase, aluminum liquid fluctuation is reduced.

As in the gas flow test the largest interface wave heights are reduced significantly for the same locations in the new type of cell compared to the waves in the conventional cell.

#### Effect of Electrolyte Level on Aluminum Liquid Fluctuation

Experiment study on the effect of different electrolyte level on

aluminum liquid fluctuation, respectively is 15cm, 16cm,

17cm, 18cm

Experimental condition : anode-cathode distance 3cm ,

aluminum liquid level 17cm , gas flow rate 1.0m<sup>3</sup>/h.

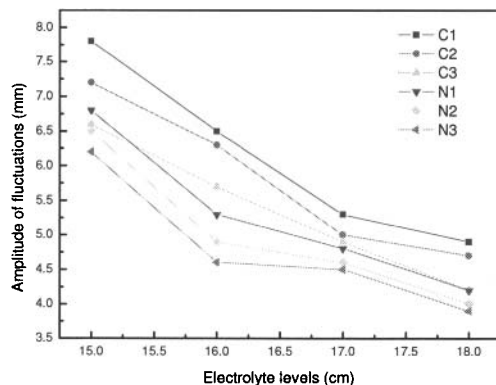


Fig. 9 Effect of Electrolyte levels on the maximum aluminum liquid fluctuation height at different points

Analysis: with the electrolyte level increase, aluminum liquid fluctuation is eased up and the maximum fluctuation height is decreased in both types of cell.

From the chart we also get C1 is above N1, C2 is above N2 and C3 is above N3. The new type of cathode structure is better than the conventional cathode structure.

#### Conclusion

We can find out the best operation parameters by the comparison of the maximum aluminum liquid fluctuation height in conventional and the new type of cathode structure electrolytic cell. With the analysis and the summary of the results, we can get the conclusions below:

(1) Under different experimental conditions, compared with the conventional cell, the maximum fluctuation height will be reduced significantly in the new type of cell. This indicates the new type of cell should have a more stable metal pad.

(2) In summary, in both conventional and new type of cathode structure electrolytic cell, the maximum aluminum liquid fluctuation height will be increased significantly along with the increasing of gas flow rate. With the decreasing of electrolyte level, the aluminum liquid fluctuation will be violent.

(3) The aluminum liquid fluctuation is extremely violent with the ACD of 3cm in both types of cell. When the anode-cathode distance increases to 4cm, the fluctuation height is reduced significantly, and the effect of the interface wave height will be reduced. In new type of cell this effect is smaller, so the anode-cathode distance can be reduced.

In conclusion, in the new type of cathode structure electrolytic cell, the largest interface wave height will be reduced effectively. The choice of anode-cathode distance is important. The decrease of anode-cathode distance will improve current efficiency. Considering the aluminum liquid fluctuation, the anode-cathode distance should not be too small, so in the new type of cathode structure electrolytic cell, the anode-cathode distance can reduce to 4cm. Within reasonable parameters the height of the electrolyte should be increased.

#### Reference

1. Feng Naixiang, Tian Yingfu, Peng Jianping et.al. *Light Metals, TMS, (2010), 406.*
2. K. E. Einarsrud, "The Minerals, "Metals&Materials Society

and ASM International”, *Metallurgical and Materials Transactions B*, 41 (2010), 560-573.

3. D. C. Chenosis and A. F. LaCamera, *Light Metals, TMS*, (1990), 211–20.
4. T. Haarberg, E. Olsen, A. Solheim, M. Dhainaut, P. Tetlie, and S. T. Johansen. *Light Metals, TMS*, (2001), 475–479.
5. W. D. Zhang, J. J. Chen, and M. P. Taylor. *CHEMCEA*, (1990), 1–8.
6. A. Solheim, S. T. Johansen, S. Rolseth, and J. Thonstad. *Light Metals, TMS*, (1989), 245–252.
7. S. K. Banerjee and J. W. Evans, *Light Metals, TMS*, (1987), 247-255.

#### **Acknowledgement**

This research was supported by the National Natural Science Foundation of China (No. 50934005) and a grant from the National High Technology Research and Development Program of China (No. 2009AA063701). National Natural Science Foundation of China (No. 50974035) National Natural Science Foundation of China (No. 51074047); the doctoral fund of EDU gov (20050145029)